UNIVERSITY
OF TRENTO

DIPARTIMENTO DI INGEGNERIA E SCIENZA DELL'INFORMAZIONE

38123 Povo – Trento (Italy), Via Sommarive 14
http://www.disi.unitn.it

ALMOST TIME-INDEPENDENT PERFORMANCE IN TIME-MODULATED LINEAR ARRAYS

L. Manica, P. Rocca, L. Poli, and A. Massa

January 2010

Technical Report # DISI-11-017

Almost Time-Independent Performance in Time-Modulated Linear Arrays

L. Manica, P. Rocca, L. Poli, and A. Massa,

Abstract

This letter deals with the optimization of the switch-on instants of the radio-frequency (RF) switches used for the synthesis of time-modulated linear arrays. It is shown that these additional degrees of freedom allow one to increase the stability of the pattern instantaneously radiated by the antenna. Representative results, obtained by means of a Particle Swarm Optimization, are reported and discussed.

Index Terms

Time Modulated Linear Arrays, Pattern Synthesis, Particle Swarm Optimization.

I. INTRODUCTION

The synthesis of time-modulated arrays considers the antenna elements equipped with a set of RF switches used to enforce a time-modulation to the static array excitations [1]. This technique has been first considered to radiate average low and ultra-low sidelobe patterns for radar applications [2]. Successively, time-modulated arrays have been proposed for wireless communication purposes (e.g., [3]). More recently, some studies have been carried out to extend the range of application of the time modulation principles to other antenna synthesis problems thus renewing the interest towards this topic. In [4], the synthesis of difference patterns has been addressed time modulating a limited number of elements of a two-section array affording a sum pattern. A theoretical analysis and a successive experimental validation on the application of time modulation to the synthesis of adaptive absorbers have been discussed in [5]. Moreover, different switching strategies have been presented in [6] to show how it is possible to suitably control the radiation patterns at harmonic frequencies.

Besides several positive features, modulating the element excitations by means of a sequence of time pulses generates undesired harmonic radiations (the so-called sideband radiations (SRs) [7]), which unavoidably affect the performance of time-modulated array antennas, thus limiting their practical applicability. To minimize the power losses in the SRs, effective approaches based on evolutionary algorithms have been proposed [8][9][10][11]. Concerning the applicability issues, a careful analysis has been carried out in [7] where suitable conditions for information transmission, and not only radar detection, have been formalized, as well.

This letter is aimed at further investigating the properties of time-modulated arrays by showing and discussing the results obtained when additional degrees of freedom are considered in the synthesis process. More specifically, the switch-on instants of the RF switches are set by means of a Particle Swarm (PS) [12] procedure to optimize the pulse sequence of the array element excitations. Starting from a synthesis problem dealing with time-averaged radiating performances, some hints on how the antenna instantaneously behaves are given.

The outline of the letter is as follows. Section 2 gives the mathematical formulation of the problem at hand and the synthesis procedure is described, as well. A set of results is reported and discussed (Sect. 3) to point out some features of time-modulated arrays marginally considered so far. Eventually, some conclusions are drawn in Section 4.

The authors are with the Department of Information Engineering and Computer Science, University of Trento, Via Sommarive 14, Povo 38050 Trento - Italy (e-mail: {paolo.rocca, luca.manica, lorenzo.poli}@disi.unitn.it; andrea.massa@ing.unitn.it)

II. MATHEMATICAL FORMULATION

The array factor of a time-modulated linear array ($TMLA$) of N-elements located along the z-axis can be expressed as [2]

$$F(\theta,t)=e^{j\omega t}\sum_{n=0}^{N-1}\alpha_n U_n(t)\,e^{j\beta z_n\cos\theta} \tag{1}$$

where ω is the carrier angular frequency, $\alpha_n=A_ne^{j\varphi_n}$ is the n-th complex excitation coefficient, and z_n is the position of the n-th element. Moreover, $\beta=\frac{\omega}{c}$ is the wavenumber of the background medium, c being the speed of light in vacuum, and θ is the angular position with respect to the array axis. The static excitation coefficients, α_n, $n=0,...,N-1$, are time-modulated by applying RF switches to the input ports of the array elements. The n-th periodic rectangular function, $U_n(t)$, $n=0,...,N-1$, of period T_p, has a value equal to $U_n(t)=1$ (i.e., the *switch-on time*) for a time step of duration $T_p\tau_n=t_n^2-t_n^1$, such that $\tau_n\in[0,1]$, $n=0,...,N-1$, and to $U_n(t)=0$ (i.e., the *switch-off time*) for the remaining part of the period. The values t_n^1 and t_n^2, $n=0,...,N-1$, are the switch-on and the switch-off instants of $U_n(t)$. Moreover, the condition $0\le t_n^1\le t_n^2$ holds true.

By expanding the periodic functions in terms of their Fourier series

$$U_n(t)=\sum_{h=-\infty}^{\infty}u_{hn}e^{jh\omega_p t} \tag{2}$$

where $u_{hn}=\frac{1}{T_p}\int_0^{T_p}U_n(t)\,e^{-jh\omega_p t}dt$ and $\omega_p=\frac{2\pi}{T_p}$, Equation (1) can be rewritten as an infinite combination of components radiated at harmonic frequencies spaced by $h\omega_p$ and centered at the carrier angular frequency ω [7]:

$$F(\theta,t)=\sum_{h=-\infty}^{\infty}e^{j(\omega+h\omega_p)t}\sum_{n=0}^{N-1}\alpha_n u_{hn}e^{j\beta z_n\cos\theta}. \tag{3}$$

Dealing with isophoric arrays having $\alpha_n=1$, $n=0,...,N-1$, the average pattern at the carrier frequency ($h=0$) is given by

$$F_0(\theta,t)=e^{j\omega t}\sum_{n=0}^{N-1}u_{0n}e^{j\beta z_n\cos\theta} \tag{4}$$

where $u_{0n}=\frac{t_n^2-t_n^1}{T_p}=\tau_n$. It is then possible to synthesize a nominal average pattern at the carrier frequency by means of a suitable choice of the τ_n, $n=0,...,N-1$, values [2][8][10]. On the other hand, the coefficients of the so-called sideband radiations ($h\neq 0$) are given by

$$u_{hn}=\frac{e^{-jh\omega_p t_n^1}-e^{-jh\omega_p t_n^2}}{j2\pi h}\ ,\ n=0,...,N-1, \tag{5}$$

and, after simple mathematical manipulations, they turn out being expressed as

$$u_{hn}=\tau_n sinc(\pi h\tau_n)\,e^{-j\pi h\left(\tau_n+2\frac{t_n^1}{T_p}\right)} \tag{6}$$

if $0\le\frac{t_n^1}{T_p}\le(1-\tau_n)$ and

$$u_{hn}=\begin{array}{c}\frac{1}{\pi h}\left\{sin\left[\pi h\left(1-\frac{t_n^1}{T_p}\right)\right]e^{-j\pi h\left(1+\frac{t_n^1}{T_p}\right)}+\right.\\ \left.+sin\left[\pi h\left(\frac{t_n^1}{T_p}+\tau_n-1\right)\right]e^{-j\pi h\left(\frac{t_n^1}{T_p}+\tau_n-1\right)}\right\}\end{array} \tag{7}$$

if $(1-\tau_n)<\frac{t_n^1}{T_p}\le 1$, respectively. As it can be observed in (6) and (7), the coefficients $u_{hn}=\mathcal{F}(\tau_n,t_n^1)$, $h\neq 0$, $n=0,...,N-1$, are function of the pulse durations τ_n, $n=0,...,N-1$, and of the switch-on instants, t_n^1, $n=0,...,N-1$.

Let us assume that the switch-on times are set to some suitable values $\tau_n=\tilde{\tau_n}$, $n=0,...,N-1$, to afford a user-defined average pattern at ω (4). As regards to the switch-on instants, t_n^1, $n=0,...,N-1$, they can be considered as additional degrees of freedom in order to optimize other properties of the antenna under analysis. For example, they are optimized by means of a PS-based strategy [12] to minimize the following functional

TABLE I

VALUES OF THE SWITCH-ON TIMES AND SWITCH-ON INSTANTS OPTIMIZED BY MEANS OF THE PS STRATEGY.

$N=16$			$N=30$		
n	τ_n^{DC}	$\frac{t_n^1}{T_p}$	n	τ_n^{SA}	$\frac{t_n^1}{T_p}$
8	1.000	0.256	1	0.065	0.599
9	0.953	0.740	3	0.076	0.461
10	0.864	0.661	4	0.072	0.583
11	0.744	0.426	5	0.065	0.815
12	0.603	0.594	6	0.880	0.514
13	0.458	0.300	23	0.965	0.823
14	0.319	0.629	27	0.171	0.580
15	0.295	0.978	28	0.473	0.000
−	−	−	29	0.976	0.812

$$\Psi\left(t_n^1\right)\Big|_{\tilde{\tau_n}} = \left\{H\left[SBL^{des} - SBL^{(h)}\left(t_n^1\right)\right]\left|\Delta_{SBL}^{(h)}\left(t_n^1\right)\right|^2\right\}\Big|_{h=1} \tag{8}$$

aimed at quantifying the matching between the sideband level[1] of the actual solution, $SBL^{(h)} = SBL\left(\omega_0 + h\omega_p\right)$, and a desired level, SBL^{des}. Moreover, $\Delta_{SBL}^{(h)}\left(t_n^1\right) = \frac{SBL^{des} - SBL^{(h)}\left(t_n^1\right)}{SBL^{des}}$ and $H(\cdot)$ is the Heaviside step function. Towards this end, a standard version of the PS, as that detailed in [13], is used because of its reliability in dealing with real unknowns.

III. NUMERICAL RESULTS

In order to evaluate the performance of the array antenna when considering the optimization of the switch-on instants, a selected set of numerical results is reported to compare the arising patterns and their time-stability. The discussion is not focused on the analysis of the time averaged performance, but it is devoted to point out the behavior of the radiated pattern at different instants within the modulating period T_p, whether the pulse-shifting is present or not. In such a case, it is still possible to consider the classical pattern features (e.g., the maximum level of the secondary lobes, SLL, the main lobe beamwidth, BW, and the peak directivity, D_{max}, [14]) for an heuristic analysis of the antenna performances. As far as the PS procedure is concerned, a swarm of 10 particles have been used and the control parameters have been set to $w = 0.4$ (inertial weight) and $C_1 = C_2 = 2$ (cognitive and social acceleration coefficients).

The first experiment deals with an antenna array of $N = 16$ elements equally-spaced of $d = \frac{\lambda}{2}$. Time modulation is used to synthesize at the central frequency, $h = 0$, an average pattern equal to a Dolph-Chebyshev pattern with $SLL = -30\,dB$. According to the result in [6], the time pulses have been chosen to start coherently (i.e., $t_n^1 = 0$, $n = 0, ..., N-1$) and the values of the normalized switch-on times have been set to the values $\tau_n = \tau_n^{DC}$, $n = 0, ..., N-1$, computed as in [15] and reported in Tab. I where, for symmetry, only half array is considered. The power losses due to the SRs [7] of such an arrangement amount to 24.2% of the total input power. As regards to the antenna behavior in correspondence with fractions of the modulating period T_p, the directivity patterns radiated at $\frac{t}{T_p} = \{0.1,\, 0.4,\, 0.7,\, 1.0\}$ are shown in Fig. 1, where the switch insertion loss present in actual feed networks is neglected. As expected, the instantaneous patterns differ from the Dolph-Chebyshev one and the antenna performances depend on the number of active elements at the sampling instant. With reference to Fig. 1, it can be noticed that starting from $\frac{t}{T_p} = 0$, when all the array elements are turned on, the efficiency of the array gets lower and lower since the elements are successively switched off. Such a monotonically decreasing behavior can be avoided by optimizing the switch-on instants, t_n^1, $n = 0, ..., N-1$, and keeping the pulse durations fixed to those of the Chebyshev distribution ($\tilde{\tau_n} = \tau_n^{DC}$, $n = 0, ..., N-1$). The PS-optimized values of t_n^1, $n = 0, ..., N-1$, are given in Tab. I. Thanks to this operation, the number of switched-on elements at each instant of T_p is kept almost constant as well as the radiated patterns (Fig. 2) . Such an event is further confirmed by the behavior of the pattern indexes in Figs. 3(*a*)-3(*b*) and related to D_{max}, SLL, and BW throughout the modulation period, respectively. For completeness, the statistics (minimum, maximum, mean values and

[1]The highest level of each h-th harmonic pattern with respect to the peak value radiated at the carrier frequency.

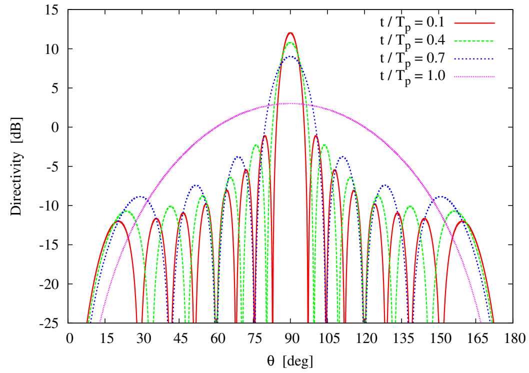

Fig. 1. *Experiment 1* ($N = 16$, $d = 0.5\lambda$) - Plots of the directivity patterns obtained at the carrier frequency when sampling the current distribution on the array aperture at $\frac{t}{T_p} = \{0.1, 0.4, 0.7, 1.0\}$ for the DC solution.

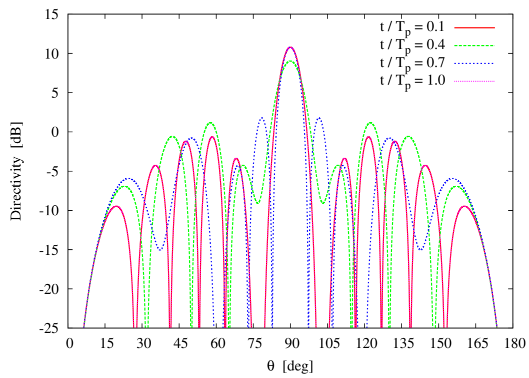

Fig. 2. *Experiment 1* ($N = 16$, $d = 0.5\lambda$) - Plots of the directivity patterns obtained at the carrier frequency when sampling the current distribution on the array aperture at $\frac{t}{T_p} = \{0.1, 0.4, 0.7, 1.0\}$ for the solution obtained by means of the PS technique.

variance) of the data in Fig. 3 are reported in Tab. II. Although the maximum available directivity (i.e., $D_{max} = 12.04\,dB$) is never achieved when using the pulse-shifting approach, it is worth noticing that the mean value is greater than that of the original case ($av\left\{D_{max}\right\}^{PS} = 10.17\,dB$ vs. $av\left\{D_{max}\right\}^{DC} = 9.47\,dB$) and, more important, the directivity value is much more stable ($var\left\{D_{max}\right\}^{PS} = 0.59\,dB$ vs. $var\left\{D_{max}\right\}^{DC} = 7.53\,dB$). Differently, the DC solution starts at $t = 0.0$ from a maximum value of the directivity, $D_{max}\left(\frac{t}{T_p} = 0.0\right) = 12.04\,dB$, while only the two central elements are "on" at $t = T_p$ when the minimum value of directivity is obtained, $D_{max}\left(\frac{t}{T_p} = 1.0\right) = 3.01\,dB$. Similar conclusions arise from the analysis of the behavior of both the SLL and the BW [Fig. 3(*b*) - Tab. II]. It is worth pointing out that the mean value and variance of the SLL of the DC solution cannot be computed when $\frac{t}{T_p} = 1.0$ (i.e., $SLL = -\infty$) because of the absence of secondary lobes. For completeness and in order to have some insights on the effects of mutual coupling (MC) interferences on the antenna aperture, the pattern obtained with the PS configuration at $\frac{t}{T_p} = 0.1$ for an array of $\lambda/2$ dipoles of radius 0.002λ is

TABLE II

Experiment 1 ($N = 16$, $d = 0.5\lambda$) - STATISTICS OF THE PATTERN INDEXES FOR THE SOLUTIONS WITHOUT (DC) AND WITH (PS) OPTIMIZED SWITCH-ON INSTANTS.

$Feature$	D_{max} $[dB]$		BW $[dB]$		SLL $[deg]$	
$Method$	DC	PS	DC	PS	DC^*	PS
$min\left\{\cdot\right\}$	3.01	9.03	6.35	6.75	$-\infty$	-12.16
$max\left\{\cdot\right\}$	12.04	10.79	59.90	9.60	-11.30	-6.66
$av\left\{\cdot\right\}$	9.47	10.17	15.57	8.07	–	-9.80
$var\left\{\cdot\right\}$	7.53	0.59	229.31	0.86	–	3.63

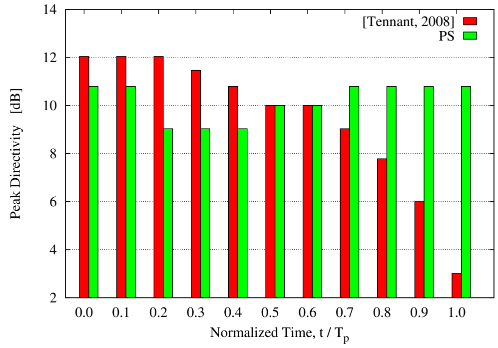

(a)

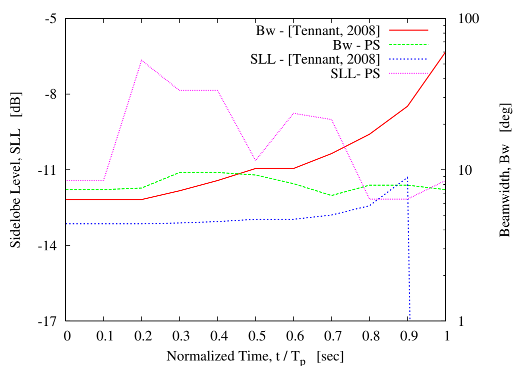

(b)

Fig. 3. *Experiment 1* ($N = 16$, $d = 0.5\lambda$) - Values of (a) D_{max} and of (b) SLL and BW for the DC solution and the solution obtained by means of the PS technique when sampling the current distribution on the array aperture at each tenth of the modulation period T_p.

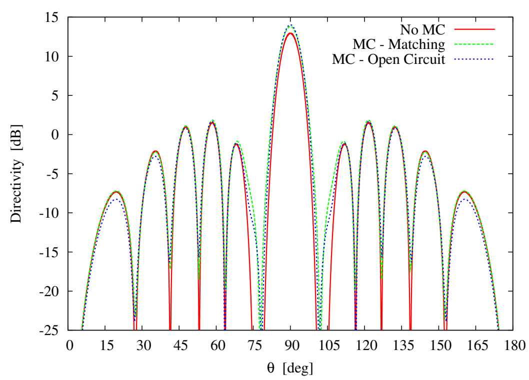

Fig. 4. *Experiment 1* ($N = 16$, $d = 0.5\lambda$) - Directivity patterns obtained for a dipole array with and without mutual coupling at $\frac{t}{T_p} = 0.1$.

reported in Fig. 4. The MC has been evaluated by considering two different impedance conditions (i.e., the perfect matching and the open circuit conditions) for the elements which are off.

In the second experiment, the same synthesis problem dealt with in [10] by means of an approach based on Simulated Annealing (SA) has been considered. A uniform linear array of $N = 30$ elements spaced of $d = 0.7\lambda$ is considered where only 9 elements of the whole architecture are time-modulated. Analogously to the previous example, the durations of the time pulses have been set to those in [10] (i.e., $\tilde{\tau_n} = \tau_n^{SA}$, $n = 0, ..., N-1$) and given in Tab. I. In this case, the percentage of power losses due to SR is 3.9%. Once again, notwithstanding the reduced number of time-controlled elements, the plots in Figure 5 and the statistics in Tab. III, assess that the optimization of the switch-on instants (Tab. I) can be profitably exploited to keep the characteristics of the radiated pattern more stable during the modulation period T_p.

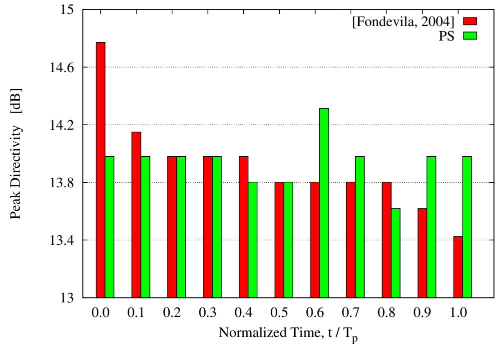

(a)

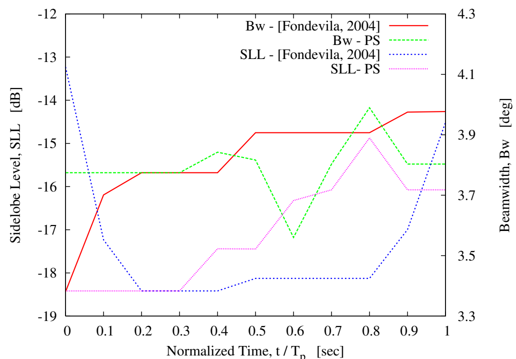

(b)

Fig. 5. *Experiment 2* ($N = 30$, $d = 0.7\lambda$) - Values of (a) D_{max} and of (b) SLL and BW for the DC solution and the solution obtained by means of the PS technique when sampling the current distribution on the array aperture at each tenth of the modulation period T_p.

TABLE III

Experiment 2 ($N = 30$, $d = 0.7\lambda$) - STATISTICS OF THE PATTERN INDEXES FOR THE SOLUTIONS WITHOUT (DC) AND WITH (PS) OPTIMIZED SWITCH-ON INSTANTS.

$Feature$	D_{max} $[dB]$		BW $[dB]$		SLL $[deg]$	
$Method$	DC	PS	DC	PS	DC	PS
$min\{\cdot\}$	13.42	13.62	3.38	3.56	-18.42	-18.42
$max\{\cdot\}$	14.77	14.31	3.98	3.98	-13.23	-14.87
$av\{\cdot\}$	13.91	13.94	3.82	3.79	-17.25	-17.09
$var\{\cdot\}$	0.11	0.03	0.03	$< 10^{-3}$	2.80	1.44

IV. CONCLUSIONS

In this letter, the effects of the optimization of the switch-on instants in time-modulated linear arrays have been analyzed and discussed. It has been shown that such an additional control positively affects the instantaneous performance of the radiation pattern. A set of results obtained through a PS-based technique has been reported to support such a conclusion.

Starting from this preliminary study, further investigations will regard the analysis of time-modulated arrays when dealing with more realistic scenarios and the presence of interference signals.

ACKNOWLEDGMENTS

The authors would like to thank Prof. R. L. Haupt for helpful discussions and suggestions. Furthermore, the authors greatly appreciated the valuable comments of the anonymous reviewers.

REFERENCES

[1] H. E. Shanks and R. W. Bickmore, “Four-dimensional electromagnetic radiators,” *Canad. J. Phys.*, vol. 37, pp. 263-275, Mar. 1959.

[2] W. H. Kummer, A. T. Villeneuve, T. S. Fong , and F. G. Terrio, “Ultra-low sidelobes from time-modulated arrays,” *IEEE Trans. Antennas Propag.*, vol. 11, no. 6, pp. 633-639, Nov. 1963.

[3] R. W. Bickmore, “Time versus space in antenna theory,” in *Microwave Scanning Antennas*, R. C. Hansen, Ed. Los Altos, CA: Peninsula, 1985, vol. III, ch. 4.

[4] J. Fondevila, J. C. Brégains, F. Ares, and E. Moreno, “Application of time modulation in the synthesis of sum and difference patterns by using linear arrays,” *Microw. Opt. Technol. Lett.*, vol. 48, pp. 829-832, 2006.

[5] A. Tennant and B. Chambers, “Time-switched array analysis of phase-switched screens,” *IEEE Trans. Antennas Propag.*, vol. 57, no. 3, pp. 808-812, Mar. 2009.

[6] A. Tennant and B. Chambers, “Control of the harmonic radiation patterns of time-modulated antenna arrays,” *Proc. 2008 IEEE AP-S International Symp.*, S. Diego, California, USA, July 5-12, 2008.

[7] J. C. Brégains, J. Fondevila, G. Franceschetti, and F. Ares, “Signal radiation and power losses of time-modulated arrays,” *IEEE Trans. Antennas Propag.*, vol. 56, no. 6, pp. 1799-1804, Jun. 2008.

[8] S. Yang, Y. B. Gan, and A. Qing, “Sideband suppression in time-modulated linear arrays by the differential evolution algorithm,” *IEEE Antennas Wireless Propag. Lett.*, vol. 1, pp. 173-175, 2002.

[9] S. Yang, Y. B. Gan, and P. K. Tan, “A new technique for power-pattern synthesis in time-modulated linear arrays,” *IEEE Antennas Wireless Propag. Lett.*, vol. 2, pp. 285-287, 2003.

[10] J. Fondevila, J. C. Brégains, F. Ares, and E. Moreno, “Optimizing uniformly excited linear arrays through time modulation,” *IEEE Antennas Wireless Propag. Lett.*, vol. 3, pp. 298-301, 2004.

[11] S. Yang, Y. B.Gan, A. Qing, and P. K. Tan, “Design of a uniform amplitude time modulated linear array with optimized time sequences,” *IEEE Trans. Antennas Propag.*, vol. 53, no. 7, pp. 2337-2339, Jul. 2005.

[12] J. Kennedy, R. C. Eberhart, and Y. Shi, *Swarm Intelligence*. San Francisco, CA: Morgan Kaufmann, 2001.

[13] M Donelli and A. Massa, “A computational approach based on a particle swarm optimizer for microwave imaging of two-dimensional dielectric scatterers,” *IEEE Trans. Microw. Theory Tech.*, vol. 53, no. 5, pp. 1761-1776, May 2005.

[14] R. J. Mailloux, *Phased Array Antenna Handbook.* Artech House (2nd Ed.), 2005.

[15] C. L. Dolph, “A current distribution for broadside arrays which optimizes the relationship between beam width and sidelobe level,” *Proc. IRE*, vol. 34, pp. 335-348, 1946.